Nonlinear microwave properties of superconducting Nb microstrip resonators

M. A. Golosovsky
Racah Institute of Physics, Hebrew University, Jerusalem 91904, Israel
and Edward L. Ginzton Laboratories, Stanford University, Stanford, California 94305

H. J. Snortland and M. R. Beasley
Edward L. Ginzton Laboratories, Stanford University, Stanford, California 94305
(Received 5 August 1994)

We present measurements of the nonlinear surface impedance $Z_S=R_S+iX_S$ of thin-film Nb microstrip resonators. We demonstrate correlation between material properties of the films and the occurrence of nonlinearity. The nonlinearity is characterized using a dimensionless parameter $r=\Delta R_S(P)/\Delta X_S(P)$. We make a short survey of the mechanisms of nonlinear electrodynamics of superconductors and demonstrate that our experimental results are best accounted for by the vortex penetration into the grains.

I. INTRODUCTION

Until recently the interest in the nonlinear properties of superconductors was based primarily on their applications as high-Q cavities in particle accelerators and frequency standards.[1–4] It was necessary to know how the properties of these cavities deteriorate at high power levels and under what conditions breakdown into the normal state occurs. Presently, superconductors find applications in microwave analog devices and the interest in their nonlinear properties has been renewed.[5–8] Very recently entirely new concepts of devices based on nonlinear properties of superconductors have appeared.[5,7] The new applications typically use thin films in microstrip or stripline geometries, which differ greatly from the geometry of the high-Q cavities used earlier. In comparison with coated cavities, the current distributions in microstrip and striplines can be highly nonuniform and may exhibit sharp maxima at the edges of the film that typically are the determining factor for the overall device performance. The key issues related to nonlinear properties of superconductors that are relevant in view of new applications include estimating the current and field levels needed to produce significant nonlinear effects and/or breakdown.

The nonlinear properties of conventional superconductors have been experimentally studied by several authors[1–4,9–11] in the context of high-Q cavity applications. These results have been systematized by Halbritter.[1] Recently, a thorough study of nonlinearities in NbN microstrip resonators was undertaken by the MIT group.[8] Their work describes the field and frequency dependence of nonlinearities but does not consider the dependence of nonlinear behavior on material parameters. For example, it has not been established why the nonlinearity was observed in microstrips made from NbN and was not observed in those made of Nb.[8] In contrast to the results of the MIT group we find that a strong nonlinearity can arise in Nb microstrip resonators depending on their material properties. We examine the relation between the nonlinearity and material properties.

The paper is organized as follows. First, we establish correlations between the occurrence of nonlinearity and material parameters of the film. Then we characterize the nonlinearity in "nonlinear" films and elucidate its mechanism.

II. EXPERIMENTAL TECHNIQUE

We studied six Nb microstrip resonators of the same total length of 4 cm and thickness $d\approx 300$ nm but with different linewidths $l\approx 40-100$ μm (hence $l\gg d\gg\lambda$ where λ is the penetration depth). We used a resonator with the inverted microstrip geometry, details of which and the experimental technique are described elsewhere.[6,7] Each resonator consists of a Nb meander line and a Nb groundplate separated by a 0.5-mil-thick Mylar dielectric. The same groundplate and dielectric were used for all resonators. The resonator was always undercoupled. Typical values for the fundamental resonant frequency of such a device were around 1.8 GHz with Q factor between 1000 and 3000 at $T=4.2$ K. The Q factor at $T=4.2$ K is determined mostly by the dielectric losses in the Mylar spacer and by radiation losses. However, at higher temperatures the losses in Nb also become observable. The thin dielectric geometry has a significant advantage over the thick dielectric setup used by MIT group[8] in that it is more sensitive to small changes in the kinetic inductance of the superconducting films.

III. EXPERIMENTAL RESULTS

A. Material characterization

The samples consist of sputtered Nb films on sapphire substrate provided by TRW, Inc. The films were patterned by contact photolithography followed by plasma etching. X-ray analysis via electron microprobe reveals no additional phases nor metallic elements. The films consist of polycrystalline Nb that is not oriented with respect to the substrate. The room-temperature dc resis-

TABLE I. Characteristics of the Nb microstriplines.

Sample	Linewidth (μm)	T_c (K)	$\frac{\rho_{300\,K}}{\rho_{10\,K}}$	$\rho_{10\,K}$ ($\mu\Omega$ cm)	Non-linearity	rf resistive tail
$D3$	40	8.94	4.2	6.2	yes	yes
$A1$	63	8.86	3.9	6.6	yes	yes
$D2$	65	8.89	3.8	6.0	yes	yes
$C3$	75	9.00	4.3	4.4	no	no
$E1$	76	8.87	4.6	3.9	no	no
$E2$	100	9.01	4.6	3.5	no	no

tivity was measured in several regions of the film by the two-point method and was found to be uniform within 10% for each film. The temperature dependence of the dc resistivity was studied by the four-point method and the results are summarized in Table I. The residual resistive ratio of all patterned films is ≈ 4 which is typical for sputtered Nb films.[1] The T_c is ≈ 9 K and does not differ much from film to film. The low-temperature dc resistivities of the films, however, do differ. We divide the samples on two groups according to their dc-resistivity values just above T_c, e.g., the films with enhanced resistivity ($D3$, $D2$, and $A1$) and those films with low resistivity ($E1$, $E2$, and $C3$) (see Table I). The dc resistivities of the films from the first group are 50% higher than those for the films of second group. As we will show, the films with enhanced dc resistivity ($D3$, $D2$, and $A1$) demonstrate strong nonlinearities, while the films with low dc resistivity ($E1$, $E2$, and $C3$) do not.

B. Microwave properties

We examine first the temperature dependence of the resonant frequency f_0 (as determined from the center of the resonance curve) and microwave losses Q^{-1} of our resonators (Fig. 1). This is done at sufficiently low power levels such that Q^{-1} and f_0 are independent of the input power. For the sake of clarity the values of Q^{-1} and f_0 at the lowest temperature, $T=4.2$ K, are subtracted. We note that Q^{-1} and f_0 for one group of the films ($E1$, $E2$, and $C3$) are fairly temperature independent except close to T_c, while Q^{-1} and f_0 for the other group ($D3$, $D2$ and $A1$) demonstrate a strong temperature dependence far below T_c. We designate this phenomenon as the "rf resistive tail."

Upon increasing microwave power the resonance curve broadens, shifts to lower frequencies and becomes asymmetric. We define the relative frequency shift as $\Delta f_0/f_0=[f_0(P_{\min})-f_0(P)]/f_0(P_{\min})$. The dependences of Q^{-1} and $\Delta f_0/f_0$ on the microwave power P are plotted in Fig. 2. For the sake of clarity the data at the lowest power are again subtracted. We observe that the films with enhanced dc resistivity ($A1$, $D2$, and $D3$, see Table I) and pronounced resistive tail (Fig. 1) demonstrate strong nonlinearities [i.e., power dependence in

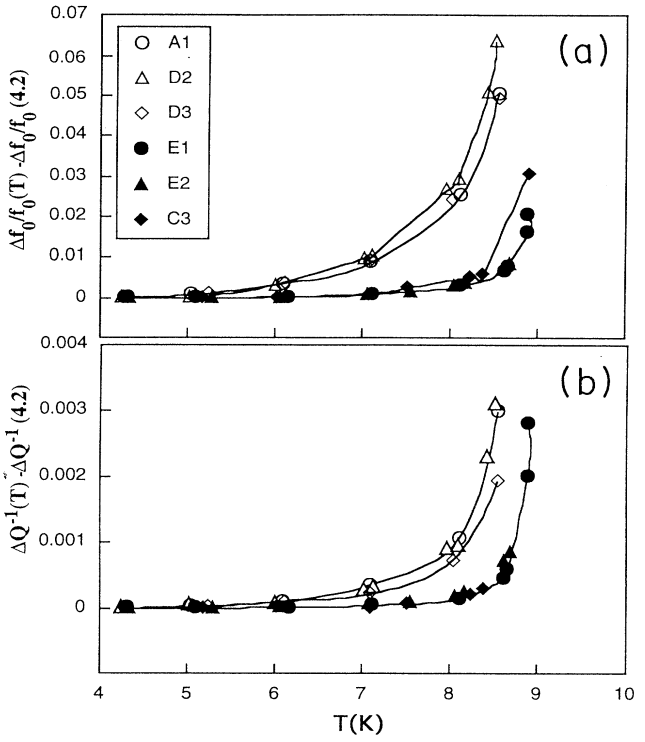

FIG. 1. Temperature dependence of (a) relative frequency shift $\Delta f_0/f_0=[f_0(4.2)-f_0(T)]/f_0(4.2)$ and (b) microwave losses $\Delta Q^{-1}=Q^{-1}(T)-Q^{-1}(4.2)$ for six Nb microstrip resonators.

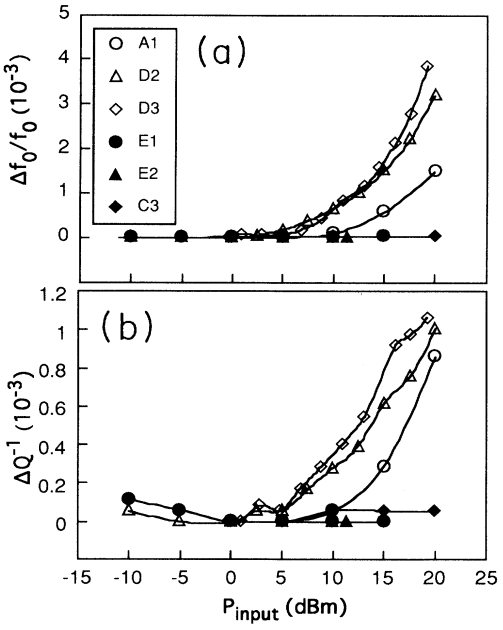

FIG. 2. (a) Relative frequency shift $\Delta f_0/f_0=[f_0(P_{\min})-f_0(P)]/f_0(P_{\min})$ and (b) $\Delta Q^{-1}(P)=Q^{-1}(P)-Q^{-1}(P_{\min})$ vs input microwave power at $T=4.2$ K. $P_{\min}=0$ dBm.

$Q^{-1}(P)$ and $\Delta f_0/f_0(P)$] over a wide range of input powers, while the films with low dc resistivity and vanishing resistive tail ($E1$, $E2$, and $C3$) show none. With increasing microwave power these latter films eventually break down, i.e., above certain threshold power the losses sharply increase so that the resonance curve no longer resembles a Lorentzian, and its width cannot be determined unambiguously.[7,8]

Nonlinearity and breakdown are independent phenomena. We conclude this from the following observation. One of our "nonlinear" samples ($D3$) was locally damaged by the electron beam during x-ray analysis. As a consequence of this damage it begun to exhibit breakdown at an intermediate input power where formerly only the nonlinearity had been seen. The nonlinearity at lower input power remained unchanged. In such a way we were able to observe breakdown and nonlinearity in the same sample.

C. Study of nonlinearity

In what follows we characterize the observed nonlinearity (Fig. 2). Figure 3 demonstrates the dependence of Q^{-1} and $\Delta f_0/f_0$ on the transmitted power P_{tr} at different temperatures for the sample $D2$. [We use here transmitted power P_{tr} and not the input power P_{in} as in Fig. 2, because for an undercoupled nonlinear resonator and coupling with loops, transmitted power is directly related to the microwave magnetic field H_{mw} ($P_{tr} \propto H_{mw}^2$), while the input power is not. We assume also that the coupling does not vary with temperature and, therefore, we can compare data for different temperatures on the same plot.] The other two nonlinear samples, $D3$ and $A1$, demonstrate similar behavior. Figure 3 demonstrates that the dependence of Q^{-1} and $\Delta f_0/f_0$ on microwave power at all temperatures except near T_c may be described by a power law, e.g., Q^{-1}, $\Delta f_0/f_0 \propto P_{tr}^n$ with $n \approx 2$ (in other words, Q^{-1}, $\Delta f_0/f_0 \propto H_{mw}^4$).

We make an important observation from Fig. 3 that upon increasing power the resonant frequency shift $\Delta f_0/f_0$ is always accompanied by the change in microwave losses Q^{-1}. Specifically, $Q^{-1}(P) \propto \Delta f_0/f_0(P)$ as demonstrated in Fig. 4(a). This linear dependence is observed at all temperatures $T < 8$ K, while at $T > 8$ K the power-law dependence $Q^{-1} \propto (\Delta f_0/f_0)^m$ with $m \approx 1.5$ holds (not shown here).

We take the slope of $Q^{-1}(P)/2$ vs $\Delta f_0(P)/f_0$ depen-

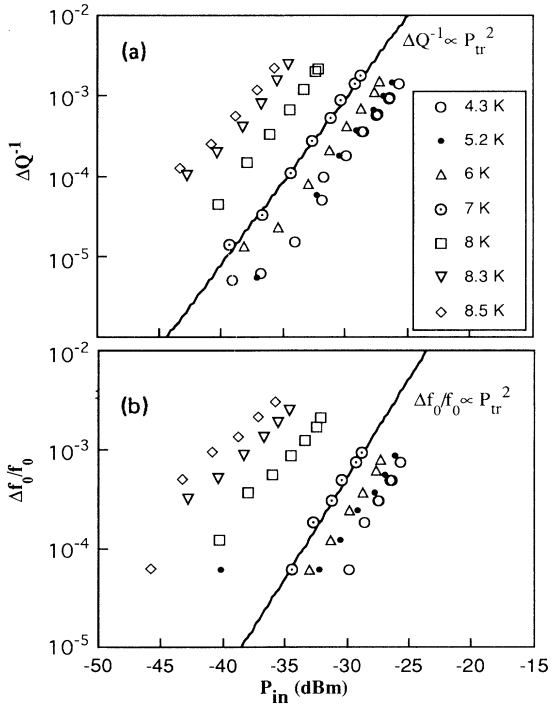

FIG. 3. Dependence of the (a) relative frequency shift $\Delta f_0/f_0 = [f_0(P_{min}) - f_0(P)]/f_0(P_{min})$ and (b) microwave losses $\Delta Q^{-1}(P) = Q^{-1}(P) - Q^{-1}(P_{min})$ on the transmitted microwave power at different temperatures for the sample $D2$. The continuous lines depict the power-law dependencies $\Delta f_0/f_0 \propto P_{tr}^2$ and $\Delta Q^{-1} \propto P_{tr}^2$; ($\Delta f_0/f_0 \propto H_{mw}^4$, $\Delta Q^{-1} \propto H_{mw}^4$).

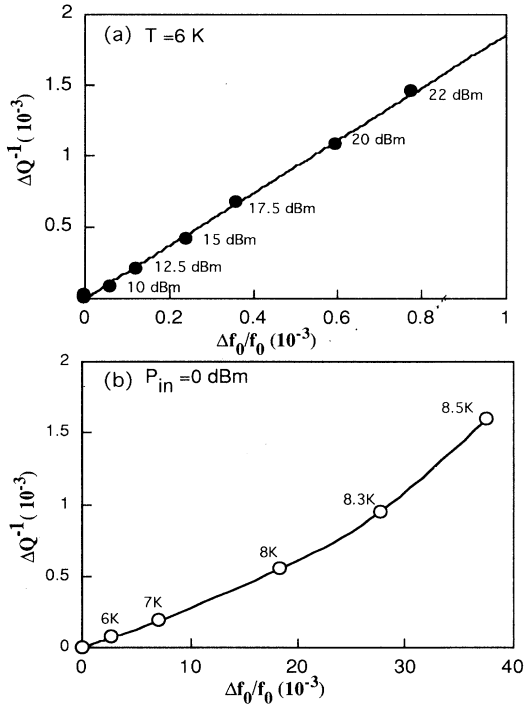

FIG. 4. (a) Q^{-1} vs $\Delta f_0/f_0$ for the sample $D2$ in the nonlinear regime as yielded from the Fig. 3. The temperature is fixed while the input power is varied. The numbers near the experimental points indicate input microwave power. The straight line shows linear approximation, $\Delta Q^{-1}/2(\Delta f_0/f_0) = 0.93$. (b) Q^{-1} vs $\Delta f_0/f_0$ for the sample $D2$ in the linear regime as yielded from the Fig. 1. The input power is fixed while the temperature is varied. The numbers near the experimental points indicate the temperature. The line is the guide to the eye. $\Delta Q^{-1}/2(\Delta f_0/f_0) \approx 0.015$. Note different horizontal scales in (a) and (b).

TABLE II. Nonlinear properties of Nb films.

Sample	Mode	Resonant Frequency (GHz)	$r=\frac{\Delta R_S(P)}{\Delta X_S(P)}$ at 4.3 K
$D3$	Fundamental	1.60	1.55
$A1$	Fundamental	1.73	0.88
$D2$	Fundamental	1.78	0.94
$D2$	3rd harmonic	5.4	0.80

dence as a figure of merit to characterize the nonlinearity. This slope is directly related to the experimentally measured quantities, i.e., to the shift of the resonance frequency $\Delta f_0(P)=f_0(P_{\min})-f_0(P)$ and to the bandwidth of the resonance curve bw, since $Q^{-1}=bw/f_0$. It can be defined also through surface resistance R_S and surface reactance X_S, since $\Delta f_0/f_0=\Gamma X_S$, $Q^{-1}=2\Gamma R_S$ where Γ is the geometrical factor. Hence, this slope is independent of any geometrical factors, characterizing specific resonator as has been noted earlier by Halbritter:[1]

$$r=\frac{\Delta R_S(P)}{\Delta X_S(P)}=\frac{bw(P)-bw(P_{\min})}{2[f_0(P_{\min})-f_0(P)]} . \quad (1)$$

The absolute values of r at 4.2 K for our samples are listed in Table II and the temperature dependence of r is plotted at Fig. 5. We note that r is fairly temperature independent except very near T_c. [Note that the data at $T>8$ K in the Fig. 5 are not well defined because the linear dependence given by Eq. (1) does not hold very well at $T>8$ K.]

We studied nonlinearities in the $D2$ resonator not only for the fundamental mode, but for higher harmonics as well. (Strictly speaking, the comparison of the data for two and more harmonics might be incorrect because the nodes and antinodes for different harmonics do not occur in the same regions of the film. This would produce a large error if the films were nonuniform. However, our dc measurements demonstrate that the films are quite uniform, so the comparison of the values of r for different harmonic makes sense in our case.) We again find that $Q^{-1}(P)\propto\Delta f_0(P)/f_0$ for a higher harmonic. We note that r at 5.4 GHz does not differ much from its value at 1.7 GHz (Table II and Fig. 5).

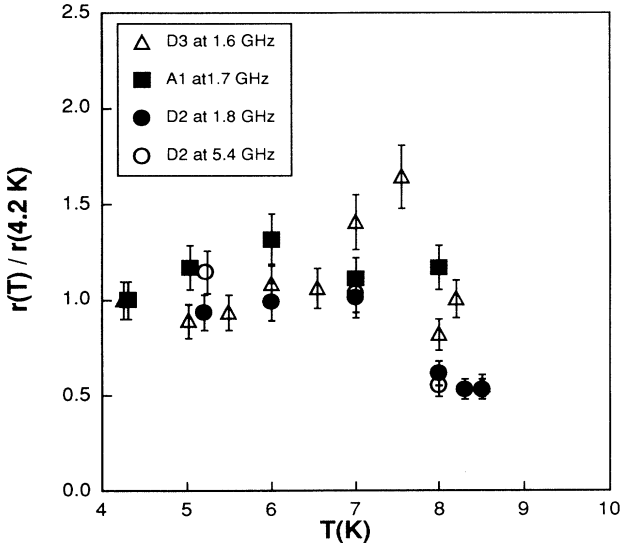

FIG. 5. Temperature dependence of the ratio $r=\Delta R_S(P)/\Delta X_S(P)$ for the samples $D2$, $D3$, and $A1$. The values of $r(T)$ are normalized to those at 4.2 K, e.g., $r(T)/r(4.2)$ is actually plotted.

D. Correlation between the occurrence of nonlinearity and material properties

From the Table I we observe that nonlinearity occurs only in those films that have simultaneously (a) enhanced dc resistivity above T_c; (b) pronounced temperature dependence of $Q^{-1}(T)$ and $\Delta f_0(T)/f_0$(rf-resistive tail); and (c) narrow linewidth.

IV. DISCUSSION

There is no universal mechanism of nonlinear electrodynamics of superconductors. Several possibilities exist and each of them may occur under certain conditions. In what follows we consider different mechanisms of nonlinearity, using the dimensionless parameter $r=\Delta R_S/\Delta X_S$ as the basis for comparison with the actual experiment. The importance of this parameter is demonstrated by our experimental observation that a change in the Q factor (e.g., surface resistance) is always accompanied by a frequency shift (surface reactance), whenever the microwave power or the temperature are changed (Figs. 1 and 2). Therefore, any explanation of nonlinearity must account for both dependences, $Q^{-1}(P)$ and $\Delta f_0(P)/f_0$. So, we compare the *absolute values* of $r(T,\omega)$ appropriate to different mechanisms of nonlinearity with the experimentally found values (Fig. 5 and Table II). Similar analysis was used earlier for the nonlinear acoustic dissipation in superconductors,[12] and recently for the field[13,14] and temperature[15] dependence of the complex impedance of high-T_c superconductors.

A. Intrinsic nonlinearity of superconductors

The existence of nonlinearities in superconductors is easily understood in the context of Ginzburg-Landau theory.[10] Parmenter[16] has derived this in terms of the BCS theory. The nonlinearity arises at large transport currents from the breaking of Cooper pairs into quasiparticles, thus affecting the complex conductivity. Parmenter obtains simple expression for the complex conductivity of the superconductor $\sigma=\sigma_1-i\sigma_2$ at a frequency ω:

$$\sigma_1=(1-K)\sigma_n , \quad (2a)$$

$$\sigma_2=\frac{K\sigma_n}{\omega\tau} , \quad (2b)$$

where σ_n is the normal-state conductivity, τ is the trans-

port scattering time of quasiparticles, and K is a dimensionless parameter depending on the current. At small current values K reduces to the two-fluid expression, $K \approx n_S/n_0$ where n_S is the concentration of the superconducting electrons and n_0 is the electron concentration in the normal state. Using the expression for the surface impedance $Z_S = R_S + iX_S = (i\omega\mu_0/\sigma)^{1/2}$ and Eq. (2) we find

$$\frac{\partial R_S}{\partial P} = \frac{\partial R_S}{\partial K}\frac{\partial K}{\partial P}\ ; \frac{\partial X_S}{\partial P} = \frac{\partial X_S}{\partial K}\frac{\partial K}{\partial P}\ , \tag{3a}$$

$$r = \frac{\partial R_S/\partial K}{\partial X_S/\partial K}\ . \tag{3b}$$

Assuming $\sigma_1 \ll \sigma_2$ (for $\omega/2\pi = 1.7$ GHz this inequality holds at $T/T_c < 0.99$) we find

$$r_{\mathrm{GL}} = \omega\tau\frac{3-K}{2K}\ . \tag{4}$$

We note that the value of r_{GL} increases with frequency and is temperature dependent (due to the temperature dependence of K and, possibly, τ). The transport scattering time in Nb in the superconducting state is temperature independent and amounts to $\tau = 10^{-12}$ sec.[17] Hence, $r_{\mathrm{GL}} \approx 10^{-2}$ at 1.7 GHz and is much smaller than the experimentally observed values (Table II). Therefore this mechanism cannot dominate in our experiments.

B. Uniform microwave heating

The superconducting film has finite surface resistance and therefore absorbs microwave power. Its temperature increases and due to the strong temperature dependence of the superconducting properties a nonlinear response might be observed. We estimate r_{heat} as follows. According to Eq. (2) both the temperature and power dependence of the complex conductivity originates from the parameter K. Thus $r_{\mathrm{heat}} = r_{\mathrm{GL}} \ll 1$ [Eq. (4)], while we observe $r \approx 1$. Therefore, our results cannot be explained by uniform heating.

We estimate independently r_{heat} from the experimental data in the linear regime. Using Eq. (3) we find

$$r_{\mathrm{heat}} = \frac{\partial Q^{-1}/2\partial T}{\partial[\Delta f_0(T)/f_0]/\partial T} \tag{5}$$

and this last value may be yielded from the data of Fig. 1. For example, in the Fig. 4(b) we plot for the sample $D2$ the dependence $Q^{-1}(T)$ vs $\Delta f_0(T)/f_0$ at constant input power that corresponds to the linear regime. We observe a monotonic dependence and determine r_{heat} using Eq. (5). We find $r_{\mathrm{heat}} \approx 0.01-0.02$ which is two orders of magnitude smaller than the value of r found in our experiment [Fig. 4(a)]. We conclude that this heating model does not account for the observed nonlinearity.

C. Weakly coupled grains model

This model was formulated first in the context of high-T_c superconductors by Hylton *et al.*[18] and has been developed in subsequent publications.[13,19,20] The model assumes the network of weak lines with uniform current flow, presumably, at grain boundaries. The nonlinearity arises from the nonlinear inductance of the weak links. We estimate $r_{\mathrm{weak\ link}}$:[18]

$$r_{\mathrm{weak\ link}} = \frac{\hbar\omega}{4eI_cR_j(1+\lambda_L^2/\lambda_j^2)}\ . \tag{6}$$

Here ω is the microwave frequency, I_c is the junction critical current density, R_j is the shunting resistance, λ_L is the London penetration length and λ_J is the effective continuum penetration length due to the network of grain-boundary junctions.[18] The absolute value of $r_{\mathrm{weak\ link}}$ strongly depends on the parameters of the grain-boundary junctions and may vary greatly. Taking typical parameters for sputtered Nb films $I_cR_j = 2$ mV,[19] $\lambda_L/\lambda_J \approx 0.5$,[18,19] we obtain $r \approx 10^{-3}$ which is much smaller than observed values. In principle, one can always find an appropriate value of I_cR_j to obtain the experimentally observed value of $r \approx 1$ (see Table II). However, the temperature and frequency dependence of r as given by Eq. (6), is incompatible with our experimental observations. For example, Eq. (6) predicts that $r_{\mathrm{weak\ link}}$ increases with increasing frequency and increasing temperature (due to the temperature dependence of I_c). We do not observe these trends. Therefore, we conclude that the nonlinearity in our experiments is not dominated by the nonlinear inductance of weak links.

D. Local heating of weak links (Ref. 21)

At high microwave current a certain weak link may be switched to the normal state. If this weak link blocks the path of the current there will be large local heating which may also drive the surrounding material into the normal state. The size of this normal-state domain depends on the microwave current. The creation of the normal-state domain may lead either to instability[22,23] or to nonlinearity.[24] According to this model the microwave power dependence of f_0 and Q^{-1} is determined by the statistics of the weak links that block the current path, while the temperature dependence of nonlinearity arises from the temperature dependence of the critical current of weak links. These weak links do not decrease T_c,[25] while they may be source of increased surface resistance[13,18,19] which appears as the rf-resistive tail (Fig. 1). The enhanced normal-state dc-resistivity in "nonlinear" films (Table I) may arise from the presence of several weak links that block the current path.

This explanation seems very appealing. However, it cannot account for the observed r values (Table II). In fact, the change of the Q^{-1} and of the resonance frequency upon formation of the normal-state domain of length L are $\delta(Q^{-1}) = (Q_N^{-1} - Q_S^{-1})L$ and $\delta(f) = (f_N - f_S)L$. For a thick film $r \approx R_N/X_N = 1$. However, our films are "thin" in the normal state. [The normal-state skin depth in our Nb films at 2 GHz is $\delta_N \approx 2.2$ μm (using dc resistivity above T_c from the Table I), the film thickness is $d = 0.3$ μm, the London penetration length in Nb is $\lambda_L \approx 0.05$ μm, hence $\delta_N \gg d \gg \lambda_L$.] So, $r \neq R_N/X_N$. We calculate r for our films using Eq. (A3) (thick-film limit) for the superconducting state and Eq. (A4) (thin-film limit) for the normal state. Then

$$r_{\text{local heating}} \approx \frac{3\delta_N^2}{2d(d-3\lambda_L)} . \quad (7)$$

Equation (7) yields $r_{\text{local heating}} \approx 170$ while we observe $r \approx 1$. Hence, we conclude that this mechanism is not responsible for the observed nonlinearity, but it might be responsible for the breakdown.

E. Vortices in weak links

This model assumes that the microwave magnetic field is so large that Josephson vortices in weak links (presumably, grain boundaries) are created. The dissipation of the microwave energy is due to the viscous drag of the vortices. The nonlinearity arises from the dependence of vortex concentration on the microwave magnetic field. This model was developed by Halbritter[1] and successfully describes the onset of nonlinearity in NbN (Ref. 8), $YBa_2Cu_3O_7$ (Ref. 20), and $Tl_2Ca_2B_2Cu_3O_x$ (Ref. 7) thin films, while it fails to describe nonlinearity at higher microwave levels in Nb and NbN thin films.[8] The model predicts almost temperature- and frequency-independent $r \leq 1$ which could be compatible with our observations (Table II). However, the fingerprint of the Halbritter model[1] is a linear dependence of R_S on the microwave magnetic field followed by saturation, which is very different from the quartic dependence, as observed in our experiments. Therefore, this model cannot fully account for our results.

F. Bulk vortex penetration (rf-critical state)

This model assumes that the microwave magnetic field is so large that vortices penetrate the bulk, not just the grain boundaries. Therefore, the magnetic flux through the sample is periodically changed. The frequency shift arises from the in-phase component of magnetic flux, while the losses arise from the out-of-phase component. Specifically, upon increasing field the vortices start to penetrate the grains when H exceeds H_{c1}. Once created, the vortices spread through the bulk and their mobility is determined by the viscous forces (at $f > 2$ GHz the viscous forces in Nb prevail over pinning forces[3,26]). Upon decreasing field the vortices leave the grains, but their motion lags after the field due to viscous forces and hysteresis occurs. The value of r for the purely hysteretic losses (with neglecting viscosity) was calculated by Granato and Lucke[27] in the context of nonlinear acoustic attenuation originating from the depinning of dislocations. They found that $r_{\text{hyst}} \approx \text{const} \sim 1$ and depends only on the geometric form of the hysteresis curve. If the effect of viscosity is dominant then the situation is similar to the normal-state skin effect for which $r = 1$. Both these possibilities are compatible with our experimental data (Fig. 5 and Table III).

We note that the hysteresis might arise not only from the trapping of the Abrikosov vortices, but also from the flux trapping in the voids and nonsuperconducting inclusions. This mechanism was proposed by Buchhold[28] to account for the nonlinear losses of Nb exposed to a low-frequency magnetic field. Such hysteretic mechanisms often show a power-law dependence of the dissipated power on magnetic field, namely, $P_{\text{diss}} \propto H^n$ with $n = 3-4$.[29] Since $Q^{-1} \propto P_{\text{diss}}/H^2$, then $Q^{-1} \propto H^{1-2}$, while we observe another dependence, $Q^{-1} \propto H^4$, which may be explained only assuming Abrikosov vortices.

The validity of the vortex penetration model in our case is bolstered by the experimental observation of the quartic dependence of Q^{-1} and $\Delta f_0/f_0$ on the microwave magnetic field (Fig. 3) in contrast to the quadratic dependence which is characteristic for intrinsic nonlinearity[10] and to the linear dependence which is characteristic for the Halbritter model.[1] This quartic dependence is compatible with the data on the nonlinear dissipation in thin as-machined Nb foils in alternating magnetic fields for which Easson and Hlawiczka[30] found a power-law dependence $P_{\text{diss}} \propto H^n$ with $n = 6$. Since $Q^{-1} \propto P_{\text{diss}}/H^2$, this corresponds to $Q^{-1} \propto H^4$ which is

TABLE III. Model predictions for the $r = \Delta R_S(P)/\Delta X_S(P)$.

Mechanism	Ref.	Q^{-1} and $\Delta f_0/f_0$ vs microwave power	r at $f = 1.7$ GHz $T = 4.2$ K	Temperature dependence of r	Frequency dependence of r
Intrinsic Ginzburg-Landau nonlinearity	16	$\propto H_{\text{mw}}^2$ (low power) $\propto H_{\text{mw}}^4$ (high power)	10^{-2}	Increases with T	$\propto \omega$
Uniform heating		$\propto H_{\text{mw}}^2$	10^{-2}	Increases with T	$\propto \omega$
Heating of weak links	21	unknown	≈ 1	T independent	ω independent
Weakly coupled grains	18	$\propto H_{\text{mw}}^2$	$> 10^{-3}$	Increases with T	$\propto \omega$
Vortices in weak links	1	$\propto H_{\text{mw}}$	≤ 1	T independent	Almost ω independent
Vortex penetration to the grains		$\propto H_{\text{mw}}^n$ with $n \approx 4$	const ~ 1	T independent	Almost ω independent

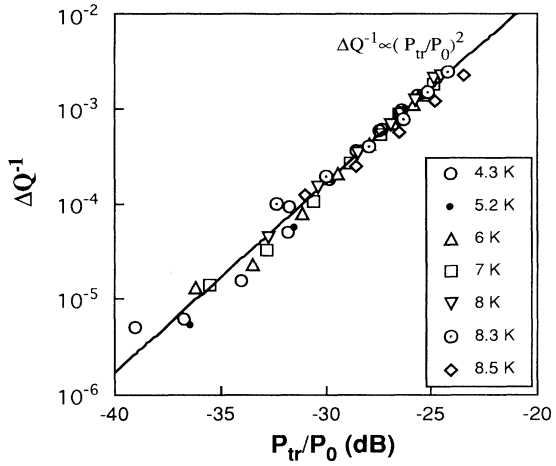

FIG. 6. Scaling of the dependence of the microwave losses $\Delta Q^{-1}(P)=Q^{-1}(P)-Q^{-1}(P_{\min})$ on the transmitted microwave power $P/P_0(T)$ at different temperatures for the sample $D2$. The data are from the Fig. 3(b). $P_0(T)$ is the scaling parameter.

very close to our observations. Easson and Hlawiczka[30] developed a generalized critical-state model that accounts for the nonlinear losses in low-frequency magnetic fields.

This model explains our results fairly well. Enhanced normal-state resistivity in our "nonlinear" films indicates a decreased field of the vortex penetration, H_{c1}[31]. We assume that the dependence of losses on magnetic field arises from the spread of H_p (field of first penetration) values in different regions of the film edges due to roughness. We assume further that our "linear" films have smoother edges. Therefore, there is almost no spread in H_p values. Upon increasing microwave power the vortex penetration suddenly occurs when H_{mw} exceeds H_p. This leads to the thresholdlike increase of the losses, in other words, to breakdown. In contrast, "nonlinear" films have a wide spread of H_p. Therefore, upon increasing power the vortex penetration occurs gradually and a strong nonlinearity is observed. In terms of this explanation the power-law dependence of the losses on magnetic field (Fig. 3) is determined by the statistics of the variation of the penetration fields at film edges. The spread of H_p is directly related to the local height variation on a rough surface which is often characterized by a power-law distribution. We yield the vortex penetration field H_p from our data as follows. The dependence of the microwave losses on microwave power (Fig. 3) at different temperatures may be collapsed to one curve by appropriate scaling $P/P_0(T)$ (see Fig. 6). This scaling is possible because the distribution of the vortex penetration fields is determined only by roughness and does not change upon varying temperature. The physical meaning of the scaling parameter $P_0(T)$ is the critical field for the vortex penetration, H_p, i.e., $P_0(T) \propto H_p^2$. In Fig. 7 we plot the temperature dependence of H_p as yielded from Figs. 3(b) and 6. We note that $H_p \propto [1-(T/T_c)^4]$ which is characteristic for H_{c1}. This dependence is compatible with the scarce microwave data for Nb (Refs. 8 and 32) and is different from that of $H_p(T)$ for NbN and $YBa_2Cu_3O_{7-x}$ as yielded from the analysis of the nonlinear microwave losses by a similar procedure.[20]

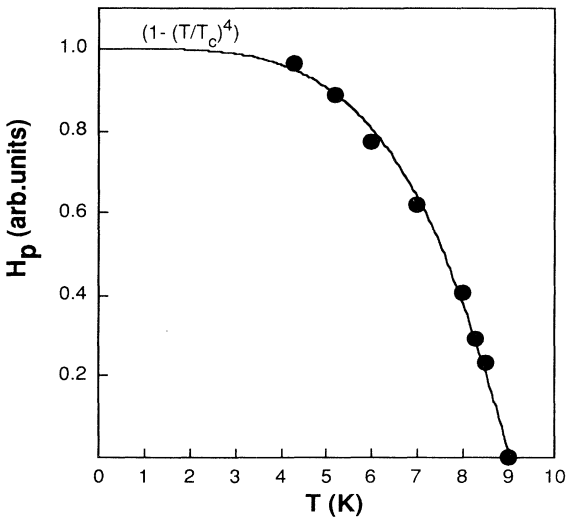

FIG. 7. Temperature dependence of the vortex penetration field $H_p \propto [P_0(T)]^{1/2}$ as obtained from the Fig. 6. The solid line shows the approximation $H_p \propto [1-(T/T_c)^4]$.

V. CONCLUSIONS

(1) The occurrence of nonlinear microwave properties in sputtered Nb thin-film microstrip resonators correlates with the enhanced dc resistivity in the normal state and with the presence of a resistive tail in the temperature dependence of the surface resistance and reactance. This correlation may be used for the prediction of nonlinear microwave properties from dc measurements.

(2) The change of the surface resistance with increasing microwave power is of the same order of magnitude as that of the surface reactance, i.e., $r=\Delta R_S(P)/\Delta X_S(P) \approx 1$.

(3) The nonlinear electrodynamics in our resonators arises from the gradual vortex penetration into the grains upon increasing microwave power.

ACKNOWLEDGMENTS

We are grateful to A. I. Larkin, R. G. Mints, L. Burlachkov, and Z. Ma for valuable discussions. We are indebted to A. M. Portis for the critical reading of the paper and constructive remarks. One of us (M.G.) is grateful to the European Community and to the Klatchky foundation for the opportunity to visit Stanford University where the experimental work was performed.

APPENDIX

Consider a microwave transmission line consisting of a superconducting strip with thickness d separated from

the superconducting ground plate with the dielectric of thickness h and of dielectric constant ε. Correction to the phase velocity due to the penetration of the electromagnetic field into superconductor is[33]

$$V_{\rm ph}(\tilde{\lambda})=\frac{V_{\rm ph}(\tilde{\lambda}=0)}{[1+(2\tilde{\lambda}/h)\coth(d/\tilde{\lambda})]^{1/2}}\ , \tag{A1}$$

where $\tilde{\lambda}$ is the complex penetration depth of the electromagnetic wave into superconductor, $\tilde{\lambda}=(1/\lambda_L^2+2i/\delta_{\rm nf}^2)^{-1/2}$.[34] Here λ_L is the London penetration depth and $\delta_{\rm nf}$ is the normal-fluid skin depth. The transmission line of finite length resonates. In the limit of $|1-V_{\rm ph}(\lambda)/V_{\rm ph}(0)|\ll 1$, the Q factor and resonant frequency shift are

$$\frac{f(\tilde{\lambda})-f(\tilde{\lambda}=0)}{f(\tilde{\lambda})}+i\frac{Q^{-1}(\tilde{\lambda})}{2}\approx-\frac{\tilde{\lambda}}{h}\coth\frac{d}{\tilde{\lambda}}\ . \tag{A2}$$

Using expansion $\coth(x)\approx 1$ for $x\gg 1$ and $\coth(x)\approx 1/x+x/3$ for $x\ll 1$, we yield in the thick-film limit, $d\gg\tilde{\lambda}$

$$\frac{\Delta f}{f}+i\frac{Q^{-1}}{2}=-\frac{\tilde{\lambda}}{h} \tag{A3}$$

and in the thin-film limit, $d\ll\tilde{\lambda}$

$$\frac{\Delta f}{f}+i\frac{Q^{-1}}{2}=-\frac{\tilde{\lambda}^2}{dh}-\frac{d}{3h}\ . \tag{A4}$$

[1] J. Halbritter, J. Appl. Phys. **68**, 6315 (1990); **71**, 339 (1992).
[2] B. Piosczyk, P. Kneisel, O. Stolz, and J. Halbritter, IEEE Trans. Nucl. Sci. **NS-20**, 108 (1973).
[3] A. Petrovich and R. M. Rose, IEEE Trans. Magn. **MAG-11**, 431 (1975).
[4] S. Isagawa, J. Appl. Phys. **52**, 921 (1981).
[5] G. J. Chen and M. R. Beasley, IEEE Trans. Appl. Supercond. **1**, 140 (1991); G. J. Chen, P. A. Rosenthal, and M. R. Beasley, *ibid.* **2**, 95 (1992).
[6] S. M. Anlage, H. J. Snortland, and M. R. Beasley, IEEE Trans. Magn. **MAG-25**, 1388 (1989).
[7] H. Snortland, X. Ma, and M. R. Beasley (unpublished).
[8] C. C. Chin, D. E. Oates, G. Dresselhaus, and M. S. Dresselhaus, Phys. Rev. B **45**, 4788 (1992).
[9] A. S. Clorfeine, Appl. Phys. Lett. **4**, 131 (1964).
[10] J. Gittleman, B. Rosenblum, T. E. Seidel, and A. W. Wicklund, Phys. Rev. **137**, A527 (1964).
[11] P. Bura, Appl. Phys. Lett. **8**, 155 (1966).
[12] Ya. M. Soifer, M. A. Golosovsky, and N. P. Kobelev, J. Low Temp. Phys. **46**, 37 (1982).
[13] A. M. Portis, D. W. Cooke, E. R. Gray, P. N. Arendt, C. L. Bohn, J. R. Delayen, C. T. Roche, M. Hein, N. Klein, G. Muller, S. Orbach, and H. Piel, Appl. Phys. Lett. **58**, 307 (1991).
[14] S. K. Remillard, M. E. Reeves, F. J. Rachford, and S. A. Wolf, J. Appl. Phys. **75**, 4103 (1994).
[15] M. Golosovsky, M. Tsindlekht, H. Chayet, D. Davidov, S. Chocron, E. Iskevitch, B. Brodskii, N. P. Bontemps, and J. P. Contour, Physica C (to be published).
[16] R. H. Parmenter, RCA Rev. **23**, 323 (1962); P. V. Christiansen, E. B. Hansen, and C. J. Sjostrom, J. Low Temp. Phys. **4**, 349 (1971).
[17] O. Klein, Phys. Rev. Lett. **72**, 1390 (1994); N. Bluzer, Phys. Rev. B **46**, 1033 (1992).
[18] T. L. Hylton, A. Kapitulnik, M. R. Beasley, J. P. Carini, L. Drabeck, and G. Gruner, Appl. Phys. Lett. **53**, 1343 (1988).
[19] C. Attanasio, L. Maritato, and R. Vaglio, Phys. Rev. B **43**, 6128 (1991).
[20] P. Nguyen, D. E. Oates, G. Dresselhaus, and M. S. Dresselhaus, Phys. Rev. B **48**, 6400 (1993).
[21] This explanation is provided by A. M. Portis.
[22] A. Vi. Gurevich and R. G. Mints, Rev. Mod. Phys. **59**, 841 (1987).
[23] A. Porch and A. M. Portis, Physica C (to be published).
[24] O. G. Vendik and H. Chaloupka (unpublished).
[25] J. R. Clem, Physica C **153-155**, 50 (1988).
[26] J. le G. Gilchrist and P. Monceau, Philos. Mag. **18**, 237 (1968).
[27] A. Granato and K. Lucke, J. Appl. Phys. **27**, 583, 789 (1956).
[28] T. A. Buchhold, Cryogenics **3**, 141 (1963).
[29] W. J. Carr, *AC Loss and Macroscopic Theory of Superconductors* (Gordon & Breach, New York, 1983).
[30] R. M. Easson and P. Hlawiczka, Br. J. Appl. Phys. **18**, 1237 (1967); J. Phys. D **1**, 1477 (1968).
[31] S. H. Autler, E. S. Rosenblum, and K. H. Gooen, Phys. Rev. Lett. **9**, 489 (1962).
[32] N. S. Shiren, R. B. Laibowitz, T. G. Kazyaka, and R. H. Koch, Phys. Rev. B **43**, 10478 (1991).
[33] R. C. Taber, Rev. Sci. Instrum. **61**, 2200 (1990), and references therein.
[34] M. W. Coffey and J. R. Clem, Phys. Rev. Lett. **67**, 386 (1991).